

A Test for the Origin of Quasar Redshifts

Piotr Popowski and Wolfgang Weinzierl

*Max-Planck-Institut für Astrophysik, Karl-Schwarzschild-Str. 1, Postfach 1317, 85741 Garching
bei München, Germany*

E-mails: popowski, weinzierl@mpa-garching.mpg.de

ABSTRACT

It is commonly accepted that quasar redshifts have a cosmological character and that most of the quasars are at Gigaparsec distances. However, there are some cases where several quasars with completely different redshifts and a nearby active galaxy are aligned in a certain way or occupy a very small patch on the sky, which is claimed by some authors to be unlikely to happen by chance. Is there a small subset of quasars with non-cosmological redshifts? For quasars apparently associated with galaxies, we consider two scenarios for the origin of their redshift: 1. a change in the scale factor of the whole Universe (standard, cosmological scenario), 2. a velocity-induced Doppler shift of a nearby object's spectrum (local, ejection scenario). We argue for a simple astrometric test which can distinguish between these two sources of quasar redshifts by constraining their proper motions.

We give the predictions for the maximum possible proper motions of a quasar for the cosmological and local scenarios of the origin of their redshifts. We apply these theoretical results to the Bukhmastova (2001) catalog, which contains more than 8000 close QSO-galaxy associations. In the standard interpretation of quasar redshifts, their typical proper motions are a fraction of micro arc-second, and beyond the reach of planned astrometric missions like GAIA and SIM. On the other hand, the quasars ejected from local AGNs at velocities close to the speed of light would have proper motions 5-6 orders of magnitude larger, which would easily be measurable with future astrometric missions, or even in some cases with HST, VLT and Keck telescope. The distributions of proper motions for the cosmological and local scenarios are very well separated. Moreover, the division corresponds nicely to the expected accuracy from GAIA and SIM.

Subject Headings: astrometry — cosmology: miscellaneous — galaxies: active — quasars: general — relativity

1. Introduction

Quasi-stellar objects (QSO, quasars) were identified as a new class by Schmidt (1963). The first object with an understood spectrum was 3C 273, with a redshift of 0.158. Many more followed

and very soon (Burbidge & Burbidge 1967) it was obvious that there are no quasars with observed blueshifts. A wavelength shift in quasars can be attributed to:

1. a cosmological redshift, i.e. due to expansion of the whole Universe (hereafter referred to as the cosmological scenario),
2. a gravitational redshift due to high concentration of material in the emission region,
3. a pure Doppler shift associated with the rapid relative motions of the system quasar-observer (hereafter referred to as the local scenario),
4. some, as of yet undiscovered, phenomenon.

Already in XIV century William Ockham realized that it is not necessary to create new entities if the explanatory potential of the known entities is sufficient — therefore, we will exclude the last possibility from the current discussion. At the first glance, the absence of blueshifted quasars strongly suggests that quasar redshifts have either a cosmological or gravitational origin. The conditions needed to produce gravitational redshifts are so extreme that we do not discuss this possibility any further. Historically, a cosmological character of redshifts was criticized based on the argument that maintaining the observed quasar fluxes requires huge energy supplies. This issue is no longer perceived as a problem, since the accretion of material on a central, super-massive black hole provides a satisfactory explanation. The Doppler (ejection) origin for quasars redshifts would be a viable alternative only if one could devise a way to avoid the blueshift problem. In the presence of only the longitudinal Doppler effect, about half of the randomly-ejected objects should be blueshifted. The situation, however, changes dramatically when the transverse Doppler effect becomes important. In this case, many of the objects approaching the observer are redshifted rather than blueshifted. Still, in a significant population of quasars, one should see a few objects that are blueshifted.

Current observational techniques have enabled well defined selection processes for QSO's. Several large area sky surveys like 2 Degree Field and Sloan Digital Sky Survey have opened a new window in the identification of QSOs and allowed the acquisition of a wealth of information (Croom et al. 2001; Schneider et al. 2002). All of the thousands of quasars that we know of are redshifted. It is unrealistic to expect that the ejection process would always meet the conditions to produce only redshifts. Therefore, a universal explanation of the redshifts of all quasars by the local hypothesis would require a giant conspiracy¹. But the ejection mechanism may be responsible for the redshifts of a subset of QSOs. There are some cases where several quasars with completely different redshifts

¹For individual quasars, the additional evidence for their cosmological redshift may come from the identification of their host galaxies in deep imaging or the detection of Lyman- α forest in their spectra. However, from the ground, the Lyman- α detections are possible only for the quasars with $z \gtrsim 1.6$ (e.g., Kim et al. 2003), which is due to the cutoff associated with atmospheric absorption.

and a nearby active galaxy occupy a very small patch on the sky, which is claimed to be unlikely to happen by chance (e.g., Arp 1999). Also, it is suggested that X-ray compact sources tend to group around nearby active Seyfert galaxies (Burbidge, Burbidge, & Arp 2003). It is even claimed by some that they preferentially lie along the minor axis of a Seyfert, and therefore were probably ejected from it (Chu et al. 1998, Arp 1999). Here we do not engage in another discussion about the significance of such cases. However, we also do not follow the route of the overwhelming majority of the astronomical community which ignores this evidence. Instead we entertain the idea of a simple astrometric test which can produce a clear, conclusive answer. We show that measuring the proper motion (μ) of QSOs or at least placing an upper limit on μ will allow one to distinguish between Doppler kinematic redshifts and the cosmological ones.

Before presenting more detailed computations, it is instructive to see why the measurements of quasar proper motions promise to distinguish between the local and cosmological origin of quasar redshifts. In the standard cold dark matter (CDM) cosmology the peculiar velocities of high-redshift galaxies, are expected to be only a tiny perturbation on top of the overwhelming Hubble flow. The same is true for quasars because they form in the centers of galaxies. Therefore, the peculiar velocities of quasars in the cosmological scenario are likely to be $v_{Q,\text{cosmo}} \sim 10^{-3}c$, where c is the speed of light. On the other hand, if the local ejections are to produce redshifts, the ejection velocities must be close to the speed of light, i.e. $v_{Q,\text{local}} \sim c$. In addition, the local quasars would be at a distance of $D_{Q,\text{local}} \sim 10$ Mpc, and the cosmological ones at $D_{Q,\text{cosmo}} \sim 1$ Gpc. Consequently:

$$\frac{\mu_{Q,\text{cosmo}}}{\mu_{Q,\text{local}}} \sim \left(\frac{D_{Q,\text{cosmo}}}{D_{Q,\text{local}}}\right)^{-1} \left(\frac{v_{Q,\text{cosmo}}}{v_{Q,\text{local}}}\right) \sim 10^{-5} \quad (1)$$

The idea of the astrometric test we present exploits this large difference between the expected proper motions. In §2 we briefly review the theory of relativistic ejection and derive some new results. Future astrometric measurements that will allow the implementation of the proper motion test are discussed in §3. In §4 we describe the catalog of QSO-galaxy associations that we use, and in §5 derive the expected proper motions of quasars in this catalog. We summarize the results in §6.

2. Theoretical considerations

We start with a brief review of the kinematics of relativistic ejection (Behr et al. 1976). We note here that the mathematical formalism of relativistic ejection can be used to describe both the local and the cosmological case. In the local scenario, a quasar is ejected with a relativistic velocity from an active galaxy. In the cosmological scenario, a quasar may be viewed as being “ejected” with its small peculiar velocity from the frame of reference moving with the Hubble flow.

We introduce a cosmological frame of reference with the observer at rest at its origin. The line connecting the observer and some point G (which may or may not represent a galaxy), defines the line of sight. A quasar Q is ejected from point G with a velocity represented by $\beta \equiv v/c$ as

measured with respect to the local cosmological standard of rest at G . The angle of ejection α in the G rest frame is the angle between the quasar velocity and the direction along the line of sight away from the observer. With these definitions one obtains for the proper motion μ of Q with respect to G ,

$$\mu = \frac{c}{D_M} \frac{\beta \sin \alpha}{1 + \beta \cos \alpha}. \quad (2)$$

where D_M is the transverse comoving distance or proper motion distance. At this point we choose standard Λ cosmology with $\Omega_M = 0.3$ and $\Omega_\Lambda = 0.7$ (e.g., Bennett et al. 2003), and set the curvature contribution to the total mass density $\Omega_K = 0$. Then the transverse comoving distance is defined as

$$D_M = D_H \int_0^z \frac{dz'}{E(z')}, \quad (3)$$

where the distance $D_H \equiv c/H_0$ is the Hubble radius², and we take the Hubble constant to be $H_0 = h \times 100$ km/s/Mpc. Under our assumptions, the function $E(z)$ (e.g., Hogg 2000) is given by:

$$E(z) = \sqrt{\Omega_M(1+z)^3 + \Omega_\Lambda}. \quad (4)$$

From (2) we see that the dependence of the proper motion on the local geometry of ejection process is described by the function $F(\alpha, \beta)$.

$$F(\alpha, \beta) = \frac{\beta \sin \alpha}{1 + \beta \cos \alpha}. \quad (5)$$

The proper motion in the cosmological scenario can be derived from Eq. (2), if we associate ejection velocity with the peculiar velocity of the quasar. In this case, we simply consider “an ejection” from the reference frame moving with the Hubble flow. For a given $\beta = \beta_0$ a maximal proper motion is achieved for the angle α_0 such that $\cos \alpha_0 = \beta_0$ and is equal to

$$\mu_{\max} = \frac{c}{D_M} \frac{\beta_0}{(1 - \beta_0^2)^{1/2}} \quad (6)$$

We assume that the peculiar velocity does not exceed $\beta_0 = (1000 \text{ km/s})/c$. This is very likely to be a conservative assumption because the pairwise velocity dispersions at $z \sim 0$ are of the order of a few hundred km/s (Jing & Börner 2001; Landy 2002) and they do not rise with z for the currently favored Λ cosmology (Barrow & Saich 1993). Hence, μ_{cosmo} is very likely smaller than:

$$\mu_{\text{cosmo}, \max} = 0.70367 \times 10^{-7} \times \frac{D_H}{D_M} h^{-1} \text{ arcsec/yr}. \quad (7)$$

²Note that in equation (3) the distance D_M is expressed in terms of the redshift z of point G , which we will approximate by the measured redshift of a quasar in the cosmological scenario or by the redshift of a galaxy in the local scenario. This approximation leads to negligible errors in the cosmological scenario, but may be important for local galaxies, since they have peculiar radial velocities that are often a substantial fraction of the radial velocity of point G with respect to the observer. In some instances, when the appropriate observational data exist, this problem may be remedied by using measured distances to galaxies instead of the ones derived from their redshifts.

The fraction D_M/D_H as a function of redshift for Λ cosmology with $\Omega_M = 0.3$ and $\Omega_\Lambda = 0.7$ is displayed in Figure 1.

In the local scenario the ejection is caused by a host galaxy. For an ejected QSO (subscript Q) and the galaxy (subscript G), Behr et al. (1976) define:

$$\kappa \equiv \frac{1+z_Q}{1+z_G} = \frac{1+\beta \cos \alpha}{(1-\beta^2)^{\frac{1}{2}}}, \quad (8)$$

where z_Q and z_G are the redshifts of the QSO and galaxy, respectively. Since a typical quasar has $z_Q \sim 2$, and a typical galaxy with which it is apparently associated has $z_G \ll 1$, the coefficient κ peaks around 3.

Our goal now is to derive the maximum possible proper motion given the angle of ejection α and coefficient κ . Eq. (8) yields

$$\beta = \frac{\cos \alpha + \kappa \sqrt{\kappa^2 - \sin^2 \alpha}}{\kappa^2 + \cos^2 \alpha} \quad (9)$$

Substitution of eq. (9) into (5) yields

$$F(\alpha, \kappa) = \frac{\sin \alpha \cos \alpha + \kappa \sin \alpha \sqrt{\kappa^2 - \sin^2 \kappa}}{\kappa^2 + 2 \cos^2 \alpha + \cos \alpha \kappa \sqrt{\kappa^2 - \sin^2 \kappa}} \quad (10)$$

We have plotted $F(\alpha, \kappa)$ as a function of α for $\kappa = 2, 3$ and 4 (Fig. 2). For each κ , $F(\alpha, \kappa)$ peaks at a characteristic angle α_{\max} given by

$$\alpha_{\max} = \begin{cases} \arccos\left[\frac{\sqrt{4-4\kappa^2+\kappa^4}}{\sqrt{4+\kappa^2}}\right] & \text{if } \kappa \leq \sqrt{2}, \\ \arccos\left[-\frac{\sqrt{4-4\kappa^2+\kappa^4}}{\sqrt{4+\kappa^2}}\right] & \text{if } \kappa > \sqrt{2}. \end{cases} \quad (11)$$

The algebraic manipulation of Eqs. (10) and (11) leads to the conclusion that the maximum observable proper motion in the local scenario is given by:

$$\mu_{\text{local},\max} = \frac{c}{D_M} \frac{\kappa}{2}, \quad (12)$$

which is a very interesting new result.

3. Astrometric Missions

The aim of this analysis is to design a test that will use the proper motions to interpret quasar redshifts. Therefore, one should consider the most powerful facilities that can make such a measurement. We limit our investigation to the upcoming astrometric missions GAIA³ and SIM⁴

³<http://astro.estec.esa.nl/GAIA/>

⁴http://planetquest.jpl.nasa.gov/SIM/sim_index.html

that are supposed to be launched around 2010. Both will reach a parallax (positional) measurement accuracy of about a few micro arc-seconds (μas) at visual magnitude $V = 15$. SIM will be able to point at tens of thousands of stars and GAIA will scan millions of stars over the entire sky. Here we describe the GAIA accuracy in some detail. We assume that SIM can reach similar accuracy with the proper integration time; moreover we expect that integration time that would allow SIM to surpass GAIA substantially will in practice be very hard to obtain. The parallax accuracy as a function of magnitude m for a mission with a GAIA-like observational setup is given by Gould & Salim (2002):

$$\sigma_{\text{par}} = \sqrt{\sigma_0^2 + \sigma_{15}^2 \times 10^{0.4(m-15)} [1 + c_{RN} 10^{0.4(m-15)}]}, \quad (13)$$

where $\sigma_0 = 2.6 \mu\text{as}$, $\sigma_{15} = 10.2 \mu\text{as}$, and $c_{RN} = 0.012$ describe the systematic-limited, photon-noise-limited, and readout-noise-limited regimes for GAIA, respectively. Gould & Salim (2002) use R as a representative magnitude. We apply the same formula to our data in V , and assume their parameters without any modification.

For N observations with uniform sampling conducted over a duration of t_E , the proper motion accuracy can be expressed in terms of σ_{par} as

$$\sigma_\mu = 2\sqrt{3}N^{-1/2}\sigma_{\text{par}}/t_E. \quad (14)$$

For the GAIA mission, it is predicted that on average $N = 82$ and $t_E = 5$ years (Zwitter & Munari 2003). The expected proper motion errors obtained by combining equations (13) and (14) are presented in Figure 3. The sampling will not be uniform for GAIA mission but formula (14) is a reasonable zeroth order approximation.

4. Data

There have been a few quasar-galaxy associations discussed individually in literature (Burbidge 1997, 1999; Burbidge & Burbidge 1997; Chu et al. 1998; Arp 1999). We have chosen a different approach and make a derivation of proper motions of a large number (8382) of close quasar-galaxy pairs from the catalog by Bukhmastova (2001). This catalog is based on the Lyon-Meudon Extragalactic Database⁵ that contains almost eighty thousand galaxies as well as the 8th edition of the Quasars and Active Galactic Nuclei catalog by Veron-Cetty & Veron (1998) that contains 11358 objects. The associations were selected requesting: (1) the availability of sky positions and redshifts for the quasars and galaxies, (2) the galaxy's redshift $z_G > 0.0004$, (3) redshift of QSO greater than the redshift of the galaxy ($z_Q > z_G$), and (4) the projected distance between the galaxy and QSO at the galaxy's redshift < 150 kpc for $H_0 = 60 \text{ km/s/Mpc}$. The Bukhmastova (2001) catalog was our only source of data throughout the analysis.

⁵<http://leda.univ-lyon1.fr/sample.html>

5. Results

Using the theoretical results from §2, we have constructed a new catalog which evaluates proper motions of quasars in QSO-galaxy associations. The complete version of this catalog, which will be published in the electronic edition of the Journal, contains 8382 lines and is composed of 9 columns. We present 20 randomly chosen entries from this catalog in the printed version of Table 1. Columns 1 and 4 give the names of the QSO and galaxy, respectively, and columns 2 and 5 the redshifts of the QSO and galaxy, respectively. In column 3 we give the visual magnitude V_Q of the QSO. These were taken directly from the catalog by Bukhastova (2001). The next four columns contain the quantities obtained by us. In column 6 we list coefficients κ [Eq. (8)]. These are followed by the maximum proper motions for the local scenario $\mu_{\text{local,max}}$ [Eq. (12)] in column 7. We list $\mu_{\text{cosmo,max}}$ [Eq. (7)] in the 8th column. Finally, the expected proper motion accuracy for GAIA mission, σ_μ [Eq. (14)], is presented in the last column. This value depends on the magnitude of a quasar, and should be also representative of the achievable SIM error. The expected GAIA (achievable SIM) accuracy is given for 7126 entries in Table 1. The remaining 1256 objects lack accuracy estimates due to one of the following reasons: either $V_Q > 20.0$ (1050 cases), which is fainter than the formal limit of astrometric missions, or V_Q was unknown (206 cases).

In Fig. 4 we present the distribution of the number of quasars with a given maximum proper motion. The left panel refers to the cosmological scenario and the right panel to the local ejection scenario. Typical proper motion in the cosmological case are $\lesssim 0.1 \mu\text{as/yr}$ and the distribution of values is rather narrow. This is a consequence of the fact that the number of quasars peaks at $z \approx 2$. The distribution of expected proper motions in the ejection scenario is wider with the proper motions expected to be typically larger than a few milli arcsec/yr and reaching 0.1 arcsec/yr in the most extreme cases.

Figure 5 illustrates the ratio of the proper motions in the cosmological and local scenarios on a quasar-by-quasar basis. Typical quasars have proper motions in the standard cosmological scenario that are 5-6 orders of magnitude smaller than those in the local scenario. This result confirms our simple expectation given in eq. (1).

In Fig. 6, we plot the number of associations as a function of the ratio of the proper motion and astrometric errors. The solid histogram presents the results for the cosmological interpretation of redshifts and the dotted histogram for the local ejection scenario. We assume $H_0 = 70 \text{ km/s/Mpc}$. The vertical thick line marks the 5σ detection limit. For the local scenario, all 7126 maximum proper motions should be detectable at the 5σ limit. Even if the proper motions are taken to be only one tenth of the maximum value, GAIA should detect 99.7% of them; if they are only one hundredth of the maximum value, GAIA should still detect 94.4% of them. Figure 2 shows that for a typical $\kappa \sim 3$, the proper motion stays within a factor of a few from the maximum proper motion for a wide range of angles α . Therefore, even if the objects have randomly distributed ejection angles which would shift the histogram toward lower signal-to-noise ratios, the proper motions should be detectable in the great majority of instances. In the cosmological case, proper motions are too

small to be detected with present or presently envisioned technology. The proper motions for only 10 quasars from our sample (0.14%) have a chance to be detected at their cosmological distances. Nevertheless, the non-detections of proper motions would undermine the kinematic interpretation of the redshifts of quasars in QSO-galaxy associations, giving support to the complete universality of the cosmological interpretation.

We warn that in some cases the apparent proper motion of quasars may be associated with their variability rather than relativistic motion of an ejected object. Such "false positives" could imply the local scenario even if the cosmological scenario is correct. Variability of a quasar is the sum of the variations coming from the continuum-producing region, broad-line region, and narrow-line region. The typical sizes of these regions are 10^{-5} pc, 0.01 pc, and 10 pc, respectively (Peterson 1997). If we assume that the sources of the quasar's light can move by the characteristic sizes of the above mentioned regions in a coherent way, then the centroid of light from a given region can move by about 10^{-3} , 1, and 10^3 μ arcsec, respectively for a quasar at a distance of 1 Gpc. Therefore, any substantial contribution to flux variability from the narrow-line region may produce spurious detection of the quasar proper motion.

6. Conclusion

We have designed a proper motion test to distinguish between the cosmological and Doppler (local ejection) origin of quasar redshifts. We considered the process of relativistic ejection and derived a new expression for the maximum proper motion given the redshift of a galaxy z_G and the redshift of an ejected object (quasar) z_Q . This maximum proper motion depends only on the redshifts z_G and z_Q and the assumed cosmological model.

Using the Bukhmastova (2001) catalog of 8382 QSO-galaxy pair associations we estimated typical proper motions for the two considered scenarios. In the standard interpretation of quasar redshifts, their typical proper motions are a fraction of micro arc-second, and beyond the reach of planned astrometric missions like GAIA and SIM. On the other hand, the quasars ejected from local AGNs at velocities close to the speed of light would have proper motions 5-6 orders of magnitude larger, and so easily measurable with future astrometric missions, or even in some cases with HST, VLT and Keck telescope⁶. The distributions of proper motions for the cosmological and local scenarios are very well separated. Moreover, the division corresponds nicely to the expected accuracy from GAIA and SIM.

We thank Greg Rudnick for a very careful reading of the original version of this manuscript

⁶The measurements with HST, VLT and Keck telescope would be probably possible only for the brightest quasars. The HST Fine Guidance Sensor reaches a per-observation precision of 1 milli arcsec for $V < 16.8$ (<http://www.stsci.edu/instruments/fgs>), and NAOS/CONICA at VLT or NIRC at the Keck telescope reach a few milli arcsec precision from the diffraction limited photometry (e.g., Genzel et al. 2003; Ghez et al. 2003).

and his helpful comments.

REFERENCES

Arp, H. 1999, *A&A*, 341, L5

Barrow, J.D., & Saich, P. 1993, *MNRAS*, 262, 717

Behr, C., et al. 1976, *AJ*, 81, 3

Bennett, C.L., et al. 2003, *ApJS*, 148, 1

Bukhmastova, Yu. L. 2001, *AZh*, 78, 675

Hogg, D. 2000, preprint (astro-ph/9905116 v4)

Burbidge, E.M. 1997, *ApJ*, 484, L99

Burbidge, E.M. 1999, *ApJ*, 511, L9

Burbidge, G., & Burbidge, M. 1967, *Quasi-stellar objects* (W.H. Freeman and Company: San Francisco)

Burbidge, E.M., & Burbidge, G. 1997, *ApJ*, 477, L13

Burbidge, E.M., Burbidge, G., & Arp, H. 2003, *A&A*, 400, L17

Chu, Y., Wei, J., Hu, J., Zhu, X., & Arp, H. 1998, *ApJ*, 500, 596

Croom, S.M., Smith, R.J., Boyle, B.J., Shanks, T., Loaring, N.S., Miller, L., Lewis, I.J. 2001, *MNRAS*, 322, L29

Genzel, R., et al. 2003, *ApJ*, 594, 812

Ghez, A.M., Salim, S., Hornstein, S.D., Tanner, A., Morris, M., Beclin, E.E., & Duchêne, G. 2003, preprint (astro-ph/0306130)

Gould, A., & Salim, S. 2002, *ApJ*, 572, 944

Jing, Y.P., & Börner, G. 2001, *MNRAS*, 325, 1389

Kim, T.-S., Viel, M., Haehnelt, M.G., Carswell, R.F., & Cristiani, S. 2003, preprint (astro-ph/0308103)

Landy, S.D. 2002, *ApJ*, 567, L1

Munari, U., & Zwitter, T. 2003, preprint (astro-ph/0306019)

Peterson, B.M. 1997, *An introduction to active galactic nuclei* (Cambridge: University Press)

Schmidt, M. 1963, *Nature*, 197, 1040

Schneider, D.P., et al. 2002, *AJ*, 123, 567

Veron-Cetty, M.-P., & Veron, P. 1998, ESO Sci. Rep., 18, 1 (<http://vizier.u-strasbg.fr/viz-bin/VizieR?-source=VII/207>)

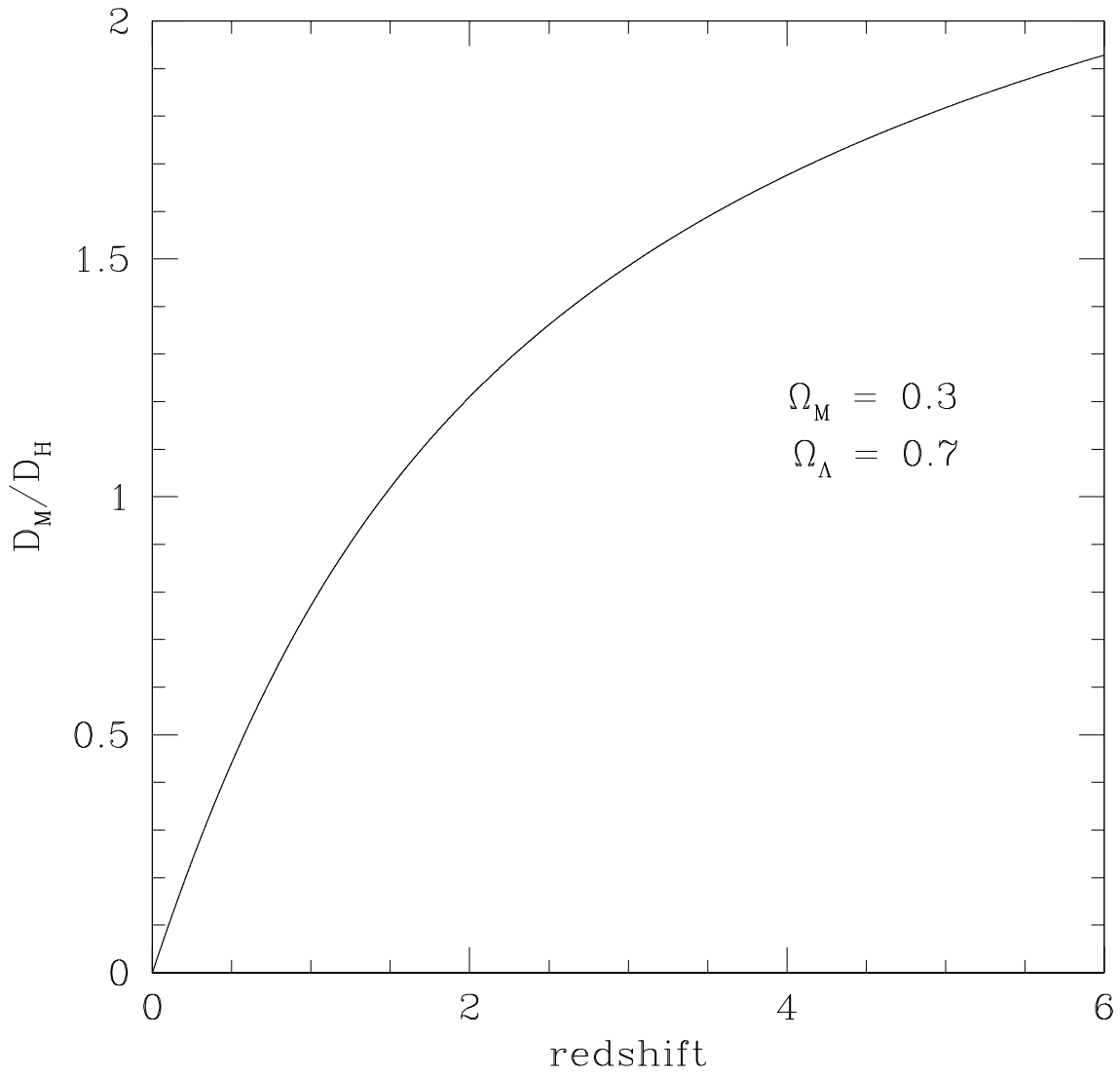


Fig. 1.— The fraction D_M/D_H as a function of redshift for Λ cosmology with $\Omega_M = 0.3$ and $\Omega_\Lambda = 0.7$.

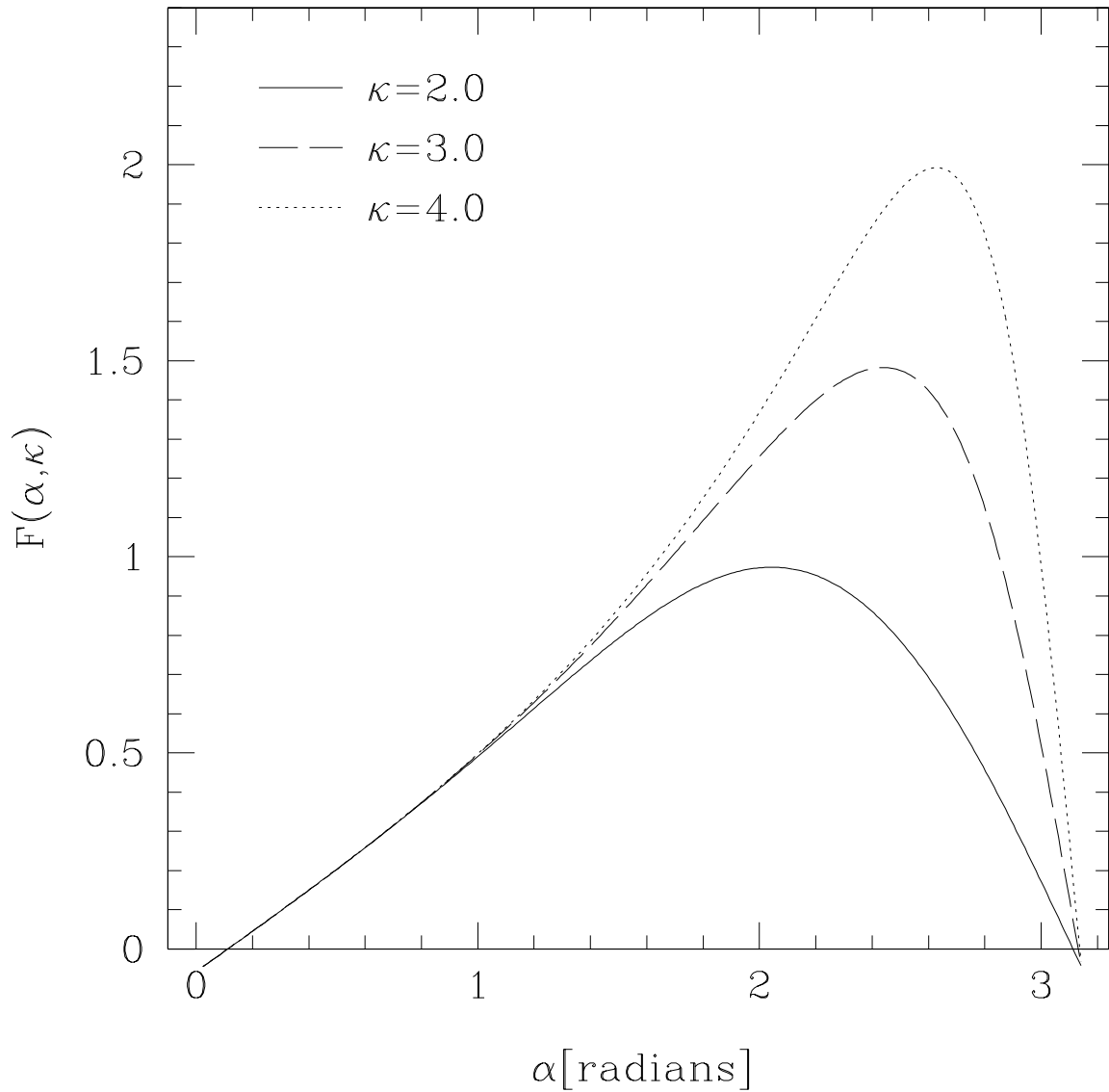


Fig. 2.— The α -dependence of $F(\alpha, \kappa)$ for $\kappa = 2, 3, 4$.

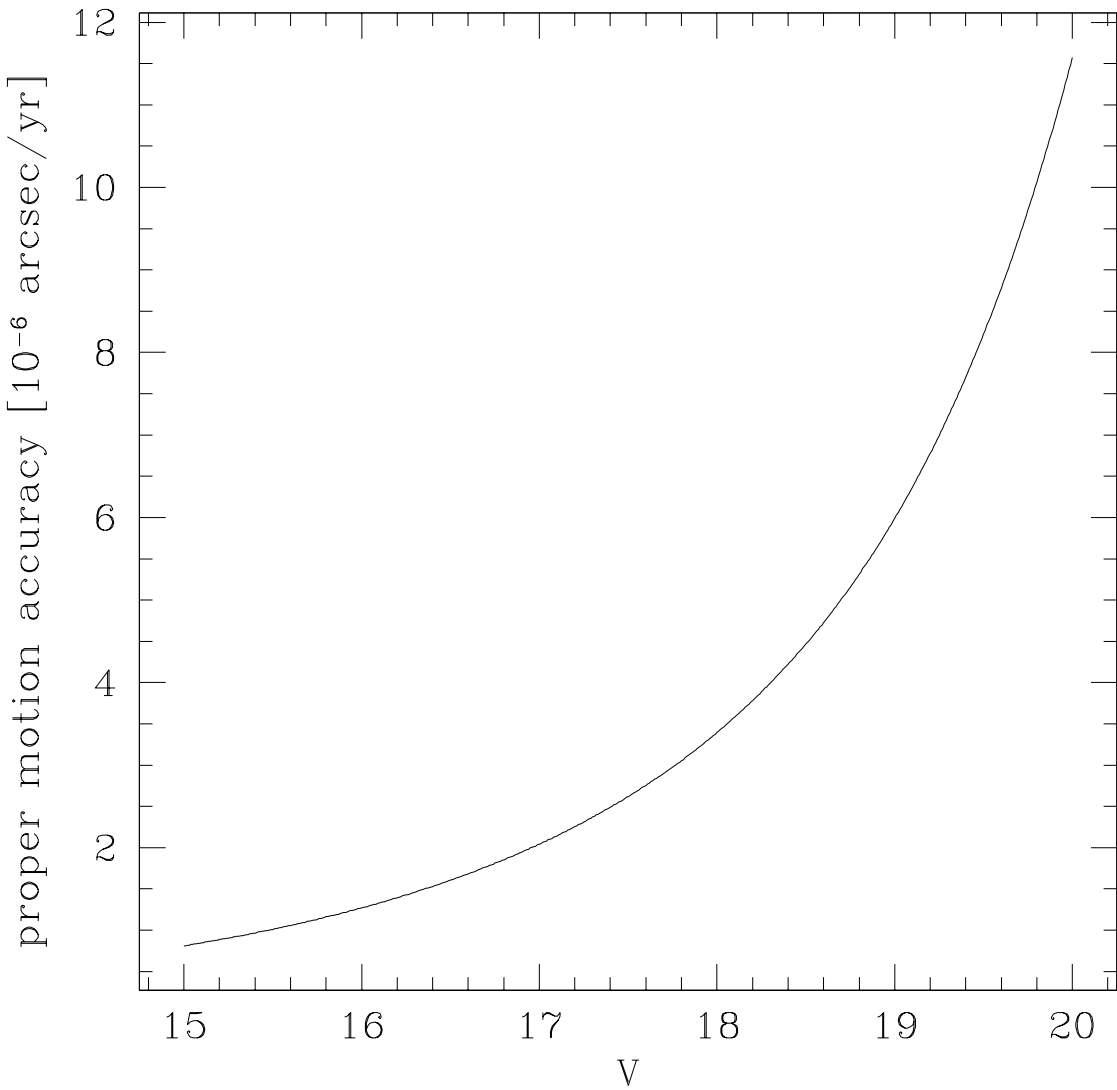


Fig. 3.— GAIA proper motion errors under the assumption of uniform sampling, the total number of observations equal to 82 and the duration of the mission of 5 years.

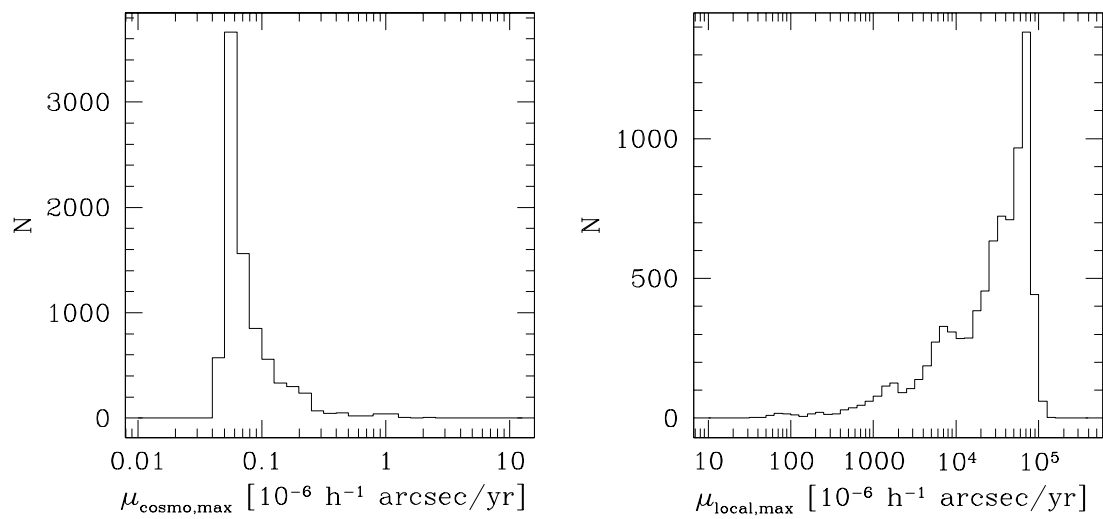


Fig. 4.— The distribution of the maximum proper motions for the quasars from the Bukhmastova (2001) catalog in two scenarios for the origin of quasar redshifts.

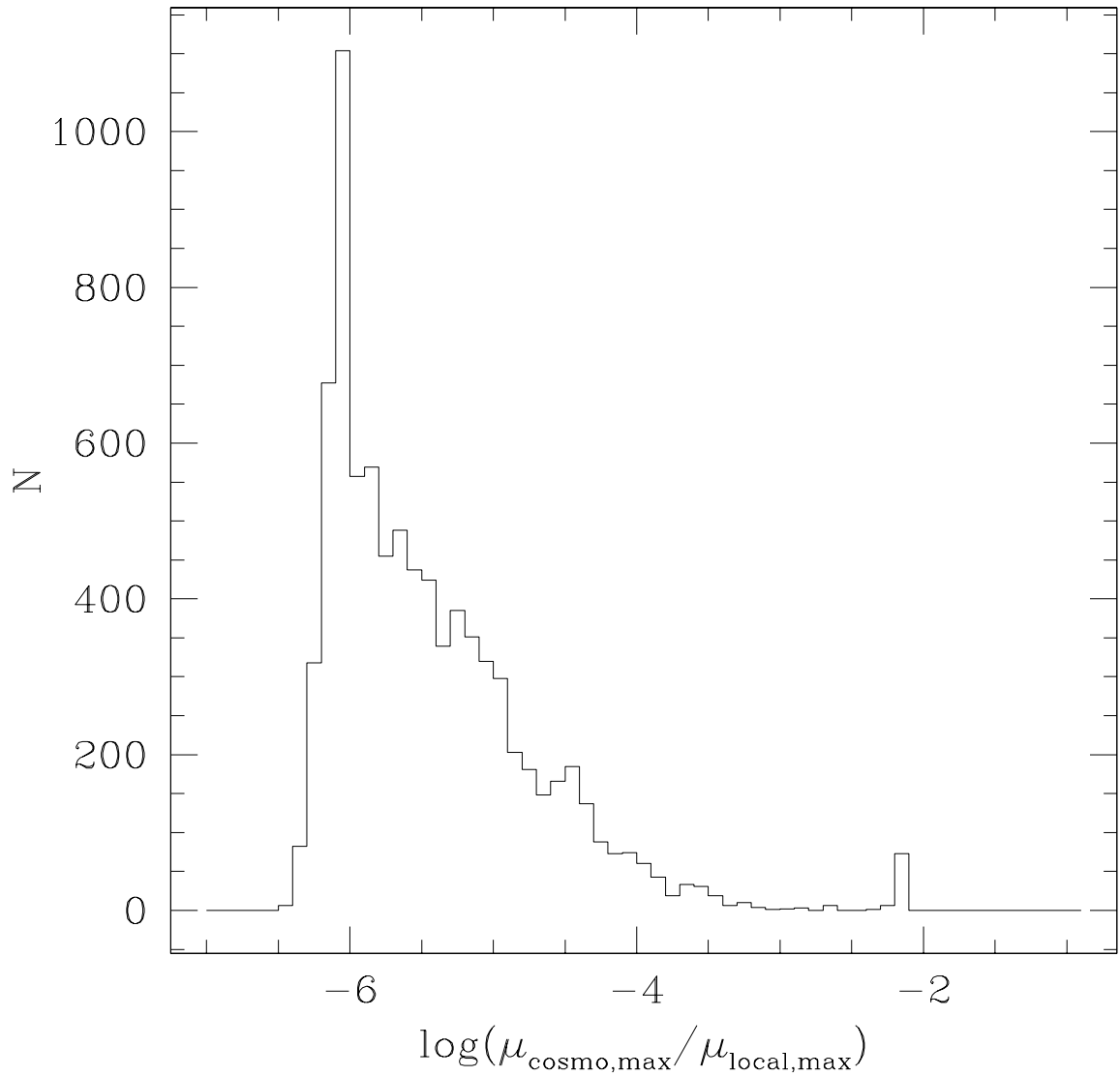


Fig. 5.— The distribution of the ratio of quasar proper motions expected from two scenarios for the origin of quasar redshifts.

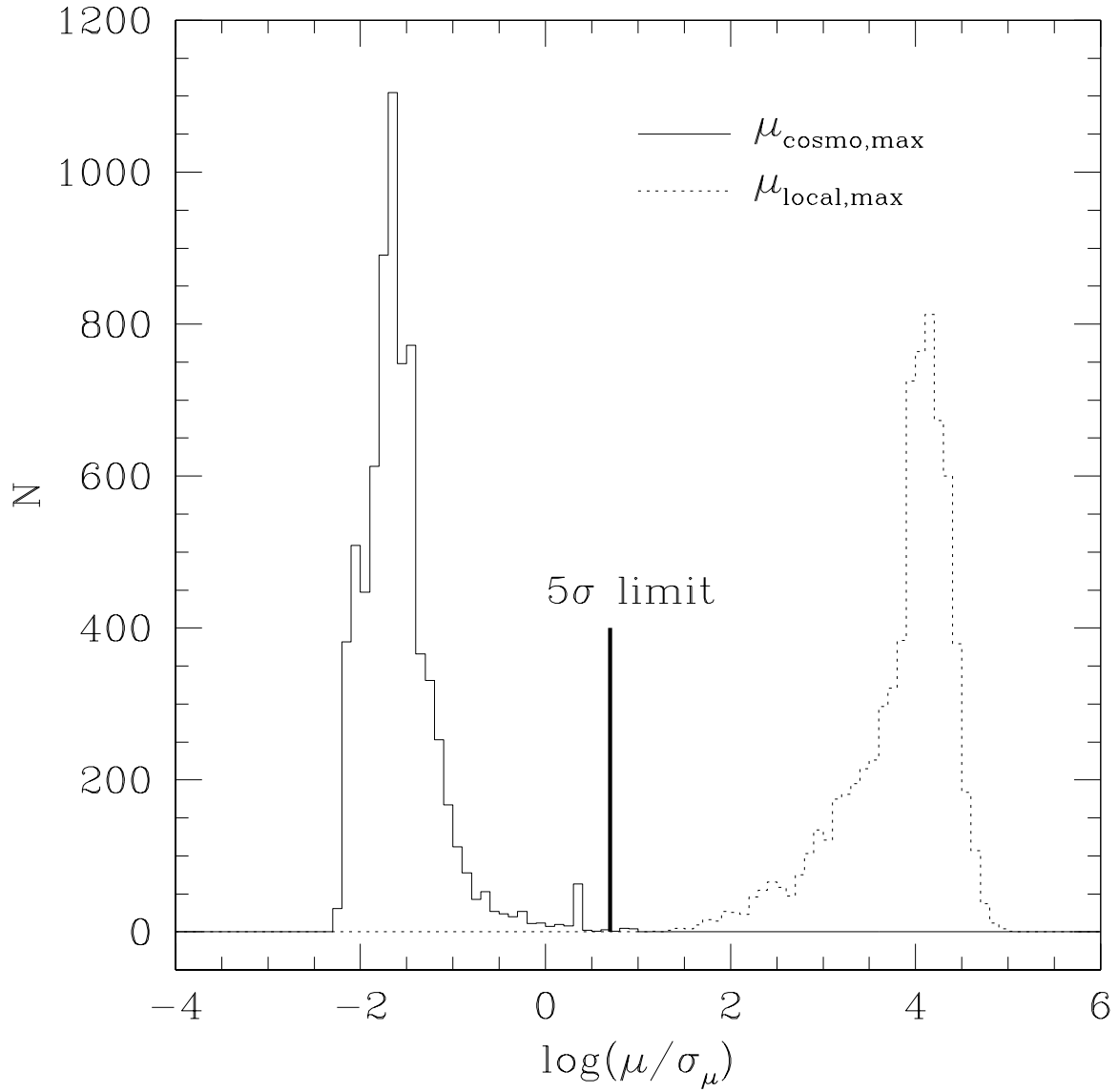


Fig. 6.— The ratios of proper motions to the errors of proper motion measurements expected from the GAIA astrometric mission. For this plot, we assumed $h = 0.7$. The solid histogram is based on the cosmological scenario and the dotted one on the local ejection scenario. The GAIA 5σ -detectability limit is marked with a vertical line.

Table 1. Proper Motions for Quasars in QSO-Galaxy Associations

Quasar	z_Q	V_Q	Galaxy	z_G	κ	$\mu_{\text{local,max}}$ [$10^{-6}h^{-1}\text{arcsec/yr}$]	$\mu_{\text{cosmo,max}}$ [$10^{-6}h^{-1}\text{arcsec/yr}$]	$\sigma_{\mu,\text{GAIA}}$ [10^{-6}arcsec/yr]
MS 23574-3520	0.5080	17.60	PGC0000621	0.0007	1.507	22707	0.157	2.76
PKS 2357-326	1.2750	18.70	PGC0073049	0.0008	2.273	29971	0.077	5.01
TEX 2358+189	3.1000	20.50	LEDA0138064	0.0024	4.090	18758	0.047	too faint
Q 2359-397	2.0300	19.00	PGC0001014	0.0004	3.029	79867	0.058	5.99
Q 0000-398	2.8270	18.80	PGC0001014	0.0004	3.825	100876	0.049	5.31
Q 0000-4244	1.7000	20.40	PGC0001014	0.0004	2.699	71169	0.064	too faint
Q 0000-4239	2.1900	21.10	PGC0001014	0.0004	3.189	84085	0.055	too faint
Q 0001-4227	2.2400	19.20	PGC0001014	0.0004	3.239	85403	0.055	6.78
Q 0001-4256	2.0300	18.80	PGC0001014	0.0004	3.029	79867	0.058	5.31
Q 0001-4225	1.3000	20.50	PGC0001014	0.0004	2.299	60625	0.076	too faint
Q 0001-4255	2.0400	18.40	PGC0001014	0.0004	3.039	80131	0.058	4.22
Q 0002-387	2.2300	19.90	PGC0001014	0.0004	3.229	85139	0.055	10.79
Q 0002-422	2.7580	17.21	PGC0001014	0.0004	3.756	99057	0.049	2.27
Q 0002-4305	2.2000	19.80	PGC0001014	0.0004	3.199	84349	0.055	10.06
87GB 00250+4458	0.9710	...	PGC0001777	0.0006	1.970	41554	0.093	...
Q 0025-4047	2.1800	17.14	PGC0001014	0.0004	3.179	83821	0.055	2.19
Q 0025-4026	1.1730	19.00	PGC0001014	0.0004	2.172	57278	0.081	5.99

Note. — The complete version of this table is in the electronic edition of the Journal. The printed edition contains only a sample.